

Experimental Investigation of Backpressure Effects on the Ionization and Acceleration Processes in a Hall Thruster

IEPC-2009-119

*Presented at the 31st International Electric Propulsion Conference,
University of Michigan • Ann Arbor, Michigan • USA
September 20 – 24, 2009*

Peng E¹, Daren Yu², and Binhao Jiang³
Harbin Institute of Technology, Harbin, Heilongjiang, 150001, China

Abstract: In order to investigate the effect of vacuum backpressure on the discharge characteristics of Hall thrusters, the atomic and ionic emission spectra and ion energy distributions are measured under various vacuum backpressures. Experimental results indicate that the vacuum backpressure decreases the electron temperature and ionization efficiency of propellants, and causes a new ionization region near the exit plane of the channel, and the penetration of the new ionization region into the channel is deeper when the vacuum backpressure is higher.

Nomenclature

A_{ik}	= Einstein coefficient for the $k \rightarrow i$ transition
α	= coefficient between propellant gas flow and backflow
e	= element charge
E_k	= energy of the excited state k
g_k	= degeneracy of the excited state k
h	= Planck constant
I	= emission line intensity
I_i	= ion current
I_i'	= ion current in the exit plane produced by accelerating the ionized mainstream
I_i''	= ion current in the exit plane produced by accelerating the ionized reflux
I_{loss}	= ion current loss
I_i^{probe}	= ion current collected by a probe
k	= constant related to the cross-sectional area of the probe and the channel
k_B	= Boltzmann constant
M	= propellant atom mass
\dot{m}_a	= mainstream flow rate
\dot{m}_b	= reflux flow rate
N_0	= number of ground state atoms per unit volume
P_b	= vacuum backpressure
S_a	= particles in mainstream ions energy distributions
S_b	= particles in backflow ions energy distributions

¹ Lecturer, Department of Electrical Engineering, Email: epengyn@163.com

² Professor, Department of Power Machinery and Engineering

³ Professor, Department of Electrical Engineering

T_e	=	electron temperature
λ	=	wavelength
η_a	=	ionization efficiency of the mainstream particles
η_b	=	ionization efficiency of the reflux particles
ν_{ik}	=	spectral line frequency of $k \rightarrow i$ transition

I. Introduction

A Hall thruster is a gas-discharging device that accelerates charged particles in orthogonal electromagnetic fields in the outer space environment. For a typical Low Earth Orbit (LEO) mission at an altitude of 400–500 km, the neutral gas backpressure is 1.3×10^{-5} Pa (about 10^{-7} Torr)¹. The ambient pressure is much lower than this for a higher altitude orbit or for interplanetary space. However, it is very difficult to simulate an actual space environment on a ground-based facility using existing vacuum technology. When a Hall thruster runs in a vacuum chamber, the backpressure is generally greater than 10^{-4} Pa, at least an order of magnitude greater than the pressure even in the LEO environment. This dramatic difference in backpressure and its effect on the operation of a Hall thruster has attracted much attention from the research community²⁻⁵.

Backpressure has two kinds of effects on the operation of a Hall thruster. One is associated with the plume, while the other is the backflow effect. The former is related to the change in the ion-atom collision rates due to the variation of background neutral gas density. This phenomenon can affect the degree of plume divergence. The latter is connected with the ionization of backflow atoms and their subsequent acceleration. Randolph determined the corresponding reference ranges of vacuum facility backpressure based on the different requirements of Electro-Magnetic Compatibility (EMC) and the far-field plume characteristics². Gallimore et al. measured the electron temperature, electron number density, ion current density, ion energy distribution, plasma potential and other plasma parameters in the far-field in a wide backpressure range by changing the number of cryopumps in operation to vary the facility pumping speed⁶. Walker found that the radial distribution of ion current density broadens and the ion number density increases with the backpressure through experiments^{4, 5}. However, Gallimore found that the background gas backflow into the channel of a Hall thruster influences the discharge behavior of plasma and the performance of the thruster^{4, 6, 7}. A pressure gradient that points to the channel is generated in a ground-based vacuum chamber, where the backpressure is relatively higher than the gas pressure inside the discharge channel, and this gradient causes the background gas to flow into the discharge channel. The background gas is ionized as a result of energetic electron impact collisions inside the channel. The ionized gas components generate a backflow that returns to the outer background by the axial acceleration electric field. If a Hall thruster runs in an “ideal vacuum,” for example, a terrestrial magnetosphere, the gas pressure gradient is very small, and can be even negative in an inverse direction from the channel to outside. The ion stream comes out from the channel and continues to defuse on the plasma pressure. The effect of backflow is therefore negligible. The ionized background gas changes the plasma density in the discharge channel through the effect of an “artificial” reflux in a ground vacuum system. In addition, the electron conduction is also affected, so that the established voltage distribution is destroyed, thereby affecting gas discharge processes such as ionization and acceleration. Walker et al. studied the effect of backpressure on the performance of a Hall thruster, and found that the proportion of anode gas (mainstream) to background gas (reflux) varies with the backpressure^{3, 4, 6}. Randolph has made a quantitative analysis on the operation parameters through the conversion of reflux “propellant” into the mainstream gas flow². It is worth noting that the heavy particles generated by exhausted ions spatter against the vacuum tank wall flow into the channel and form non-conducting coatings on the anode and the insulators⁸. The deposition of the non-conducting coatings is subject to the influence of backpressure, but special anti-sputtering coatings can be applied on the inner wall of the vacuum chamber to avoid the effect of ion sputtering.

It can be seen from the presentation above that much progress has been made in studying the characteristics of plumes, and a good foundation has been laid for the analysis of the interaction between spacecraft and thruster. However, not much work has been done so far on the physical processes involved in the flow of vacuum neutral gas into the channel. It is therefore of great significance to analyze the ionization and acceleration processes of the working gas, and the corresponding physical conditions for various backpressure.

Ion acceleration depends to a high degree on the ionization process of the working gases⁹. In order to investigate the effect of backpressure on the discharge characteristics of Hall thrusters, we used a P70 Hall thruster

to study the physical processes of ionization and ion acceleration. We used a multi-grid probe and a spectrometer to measure the distributions of ion energy in the far field, and the electron temperature along the channel, respectively. In the remainder of this paper, the experimental setup is described in Section II, experiment results and analysis are presented in Section III, conclusions are drawn in Section IV.

II. Experimental Devices

A. Experimental Thruster

A thruster of P70 type was used as the experimental thruster is as shown in FIG. 1. The numbers of turns in the outer, inner and trim coils are 74, 146, and 57, respectively.

B. Vacuum Facility

The experiments were performed in a stainless steel chamber of 1.5 m in diameter and 4 m in length, shown in FIG. 2. The chamber was equipped with two diffusion pumps with a pumping speed of 14,000 l/s for air. Under the operating conditions, the dynamic pressure was 2.0×10^{-2} Pa when the thruster was operated with krypton gas at a mass flow rate of 2 mg/s. The vacuum gauge was calibrated for krypton gas. In order to increase the background pressure for this study, extra Kr gas was allowed to flow into the chamber. For the high pressure case, an extra 2 mg/s is fed into the chamber behind the thruster to raise the background pressure to 4.2×10^{-2} Pa.

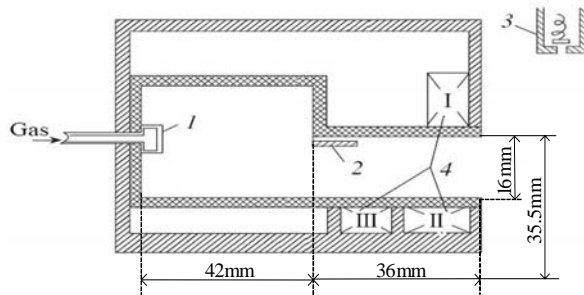


Figure 1. Schematic of the P70 Hall thruster. 1: gas distributor, 2: anode, 3: cathode and 4: magnetic coils (I-outer coil, II-inner coil, III-trim coil).



Figure 2. Vacuum facility

C. Measurement Apparatus

The measuring apparatus used in the experiments include an Ava eight-channel raster spectrometer and a multi-grid probe.

The spectrometer has a measurement range from 200 nm to 1200 nm and a resolution better than 0.1 nm. Measurements were made only between 350 nm and 1000 nm because of the sensitivity range of the spectrometer detector. To reduce noise and to prevent signals from being saturated, the measuring integration time was chosen to be 100 ms. In order to reduce the impact of optical bandwidth on the spectral radiation magnitude, a collimation lens of 6 mm in diameter was fixed in the forward part of the receiving optical fiber, so that, only parallel light of 6 mm in diameter can be processed by the spectrometer, to ensure the measurement precision. For easy collection of the emission spectrum from inside the channel, a slot of 10.5 mm long and 8 mm wide was cut as shown in FIG. 3. For the purpose of avoiding sputter on

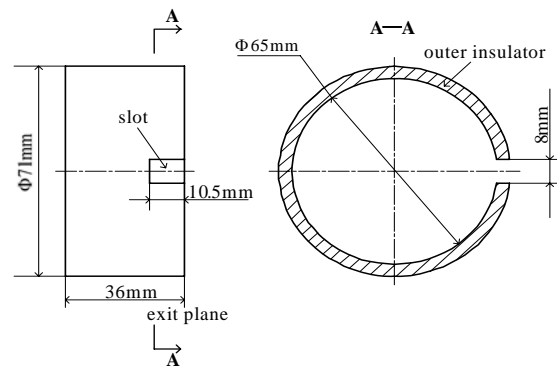


Figure 3. The slot cut in the outer insulator near the exit plane

the collimation lens and reducing the perturbation of plasma by the probe itself, a ceramic sleeve of 20 mm long, 6 mm in outer diameter and 4 mm in inner diameter was connected to the collimation lens. The axial position of the fiber optic probe can be controlled by a stepper motor with a measurement step of 0.5 mm. In order to reduce the measurement errors, five sets of spectral line intensity data were collected at each point, and the mean value was calculated with error bars. It should be noted that the spectrometer was calibrated before the air in the chamber was evacuated..

TABLE1. Experimental conditions

case	discharge current	biased voltage (C2)	vacuum backpressure
1	3.16A	-18V	2.0×10^{-2} Pa
2	3.49A	-17V	3.0×10^{-2} Pa
3	4.02A	-17V	4.0×10^{-2} Pa

The multi-grid probe was constructed by grids C1, C2 and collector K is as shown in FIG. 4. A biased negative voltage tabulated in TABLE. 1 was applied between C2 and C1 to cut off the electron current, and then the ionic current vs. voltage can be measured by changing the biased positive voltage of up to 400 V imposed on K. Before the experiments, the radial position of the probe center was adjusted to keep it in line with the central axis of the discharge channel. The distance between C1 and the exit plane of thruster was set to be 70 cm to reduce the plume impact on the probe.

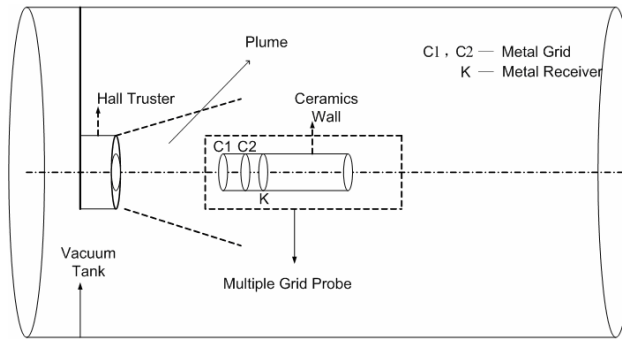


Figure 4. Installation of multi-grid probe in vacuum tank

III. Experimental Results and Analysis

Our study was carried out at a discharge voltage of 400 V, an anode krypton flow rate of 2 mg/s, and a cathode krypton flow rate of 0.3 mg/s. The magnetic coils were separately supplied by three power sources, and were used to regulate the magnitude of excitation currents until the discharge current was minimized. The excitation currents measured at the outer, inner and trim coils were 4.16 A, 3.32 A and 1.74 A, respectively. The experiments were conducted at 2.0×10^{-2} Pa, 3.0×10^{-2} Pa and 4.0×10^{-2} Pa with an additional adjustable flow of Kr gas fed into the vacuum chamber.

A. Energy distribution of exhausted ions with background gas discharge taken into consideration

It can be seen from FIG. 5 that the V-I curves are similar in shapes. In order to analyze the trend of these curves, each of them is divided into the following four parts:

- 1) Region I (Platform): This part of the ion current comes from the acceleration of mainstream and reflux ions, and the width of this platform is decided by the mean energy of ionized reflux;
- 2) Region II (Backflow): The drop in ion current in this region is caused by the energy distribution of ionized reflux;
- 3) Region III (Transition): This part is only a small portion of the total ion current composed of a few high-energy ionized reflux particles and low-energy primary ions, with a relatively wide energy spectrum; and
- 4) Region IV (Mainstream): The ion current in this region tends to decrease more rapidly than that in region II, which is caused by the energy distribution of ionized mainstream.

It can be seen from FIG. 6 obtained through differentiation, linear interpolation and filtering that the energy distribution curves have two distinct peaks. The minor and major peaks represent low- and high-energy ions, which are related to the ionized mainstream and reflux particles, respectively. It can also be seen that the energy of the ionized background gas obtained from the axial electric field is lower than that of the ionized anode gas, and the former flux is smaller than the latter flux. The peak of ionized anode gas does not decrease significantly with the increased backpressure, which suggests that the variation of backpressure has only a slight effect on the primary ions. The peak of the ionized reflux gas is higher and the corresponding energy increases with the backpressure. This effect indicates that with the increase of the backpressure, more energy can be obtained from the accelerating electric field for the same ionized backflow, and the ion flux increases correspondingly. The changes in the performance of a Hall thruster, such as thrust and specific impulse caused by backpressure have been confirmed by the work done by Gallimore et al^{3,4,6}.

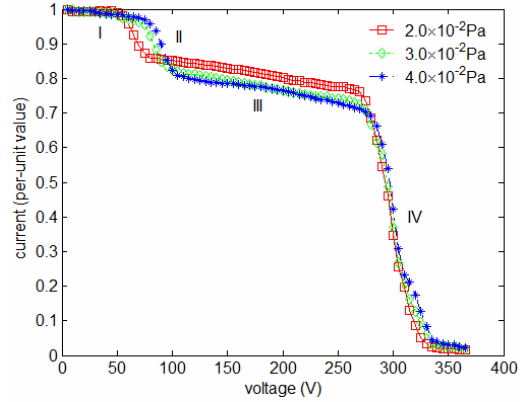


Figure 5. V-I curves measured by multi-grid probe under various vacuum backpressures

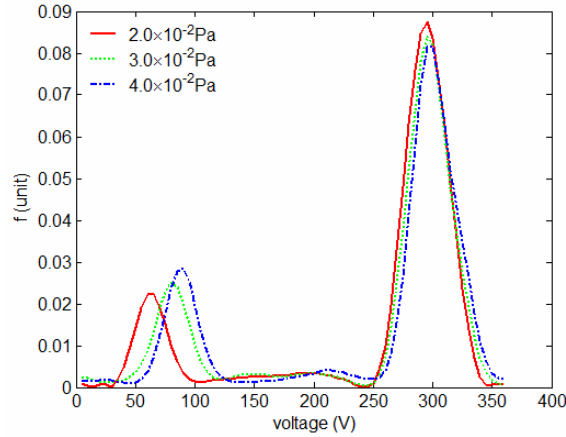


Figure 6. Ion energy distribution under various vacuum backpressures

It can be seen from the analysis of the energy distributions of exhausted ion above that the changes in backpressure exert the greatest impact on the ionized background gas flow and their energy distribution.

The ionized background gas flow depends largely on its density and energy. Since the energy of the ionized reflux is relatively low and more or less constant mainly in the range of 60~100 eV, the variation of ionized background gas flow caused by backpressure is primarily due to the changes in the number density of the ionized reflux. Therefore, it is necessary to analyze the relationship between the reflux flow rate and the backpressure.

The ion current collected by a probe can be expressed as:

$$I_i^{probe} = k [I_{i'}(\dot{m}_a, \eta_a) + I_{i''}(\dot{m}_b, \eta_b) - I_{loss}(P_b)] \quad (1)$$

where k is a constant related to the cross-sectional area of the probe and the channel, as well as the plume divergence angle, $I_{i'}$ and $I_{i''}$ are the ion currents in the exit plane produced by accelerating the ionized mainstream gas and reflux particles, respectively. These are not only determined by the flow rate of the mainstream/reflux particles represented by \dot{m}_a and \dot{m}_b , respectively, but also by the ionization efficiency of the mainstream/reflux particles represented by η_a and η_b , respectively. The parameter I_{loss} represents the ion current loss due to the collisions between the exhausted ions and the background gas atoms and is related to vacuum backpressure P_b .

Assuming that the collisions between the exhausted ions and the background gas atoms are elastic, and that the collision cross-section is independent of the speed of the exhausted ions, the ion currents of ionized mainstream and reflux gas particles lost between the exit plane and the collecting surface of the probe represent the same portion of

each to the total ion current. Therefore, coefficient α , which represents the ratio of the corresponding energy distribution area for the ionized mainstream and reflux particles shown in FIG. 6, can be used to express the ratio of I_i' to I_i'' , as:

$$\alpha = \frac{S_a}{S_b} = \frac{I_i'}{I_i''} \quad (2)$$

where S_a and S_b are the corresponding particles in mainstream and backflow ions energy distributions, respectively. It should be pointed out that the integrals for the particles are calculated for the area with 5% of their respective peak value and up. It can be seen from FIG. 6 that α becomes smaller with the increasing backpressure, which means that the ion current of the ionized reflux detected by the probe represents a larger portion of the total current.

Ion current I_i can usually be expressed as:

$$I_i = \frac{e}{M} \eta \dot{m} \quad (3)$$

where e , M , η and \dot{m} denote element charge, propellant atom mass, ionization efficiency and propellant mass flow rate, respectively.

Assuming that the mainstream and reflux are fully ionized, namely $\eta_a = \eta_b = 1$. From Eqs. (2) and (3),

$$\alpha = \frac{\dot{m}_a}{\dot{m}_b} \quad (4)$$

According to FIG. 6 and Eq. (4), the reflux flow rate \dot{m}_b can be obtained, and its percentage in $(\dot{m}_a + \dot{m}_b)$ varies with backpressure as shown in FIG. 7.

It can be seen from FIG. 7 that the reflux flow rate increases with the backpressure, and the percentage of the reflux flow rate in the whole flow rate increases from 13% to nearly 20% for backpressures in the range of $2.0 \times 10^{-2} \sim 4.0 \times 10^{-2}$ Pa. It can therefore be concluded that the backpressure has a significant effect on the reflux in this pressure range. It is also noted that the electron temperature near the exit is lower than that in the main ionization zone, so the backflow ionization efficiency η_b is probably smaller than the mainstream ionization efficiency η_a , and the exact reflux flow rate may be larger than the calculated result above.

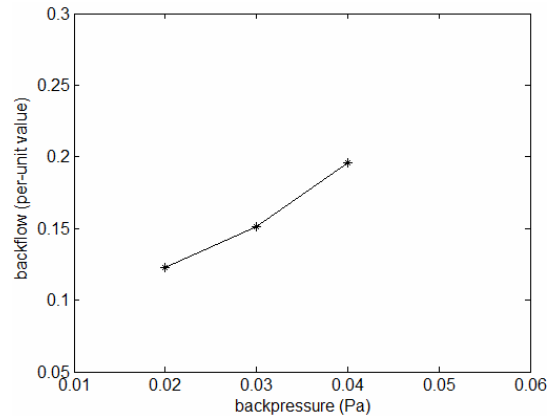


Figure 7. Reflux flow rate under various vacuum backpressures

The energy distribution of the ionized reflux flow mainly depends on the energy level of the ionized reflux particles acquired from the accelerating electric field. If it is assumed that the backpressure does not influence the plasma potential distribution in the channel. Therefore, there is a one-to-one correspondence between the energy level of ionized reflux particles and their ionization position, namely the depth of the backflow induced into the discharge chamber.

B. Penetration of background gas flow into thruster channel

Since most of the ionized particles in the channel are univalent ions, and according to the basic rule that the particle density is proportional to the corresponding spectral line intensity, two spectral lines, with relatively high intensity, can be chosen from the univalent ion lines (Kr II) to investigate the ionization behavior of the backflow in the channel. The two univalent ion lines with wavelengths of 966.33 nm and 989.30 nm, corresponding to $4p^4(^3P)5p(^4S_{3/2}^o) \rightarrow 4p^4(^3P)4d(^2P_{3/2})$ and $4p^4(^1D)4d(^2P_{3/2}) \rightarrow 4p^4(^3P)5p(^4S_{3/2}^o)$, respectively¹⁰, can be measured along the channel axis, as shown in FIG. 8.

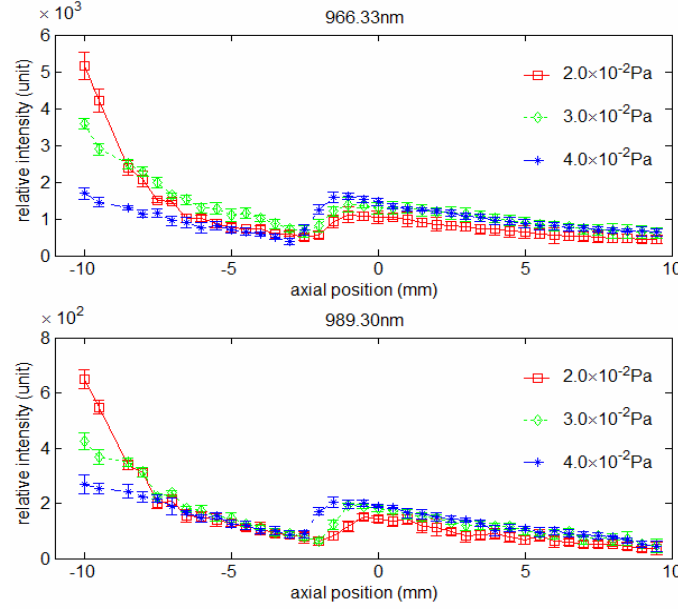


Figure 8. Axial distribution of KrII spectrum intensity under various vacuum backpressures (Reference point “0” denotes the exit plane of the thruster, the left and the right sides refer to the anode and far field direction, respectively, and the same is referred to other figures below.)

It can be seen from FIG. 8 that:

- 1) The vacuum backpressure increases as the ion spectral line intensity decreases.
- 2) A peak caused by the ionization of reflux particles appears near the exit, and the axial location of this peak can be regarded as the ionization zone of the reflux. The peak intensity increases with backpressure, which means that the number density of ionized reflux atoms increases with the increase of backpressure, thereby enhancing the local plasma density.
- 3) The penetration of the background gas flow into the channel increases with the backpressure. This means that the mean free path of the background gas atoms in the channel becomes longer as the backpressure increases. Usually, the mean free path of the atoms becomes longer as the local electron density and electron temperature decrease. However, it appears that the mean free path of the background gas atoms increases with electron density for a higher backpressure, and therefore, it is necessary to do further analysis of the changes in electron temperature with backpressure.

C. Effect of Background gas flow on distribution of electron temperature

According to atomic spectrum theory, the emission line intensity of an atom ($k \rightarrow i$ transition) can be expressed as¹¹:

$$I_{ik} = N_0 g_k A_{ik} h \nu_{ik} e^{-\frac{E_k}{k_B T_e}} \quad (5)$$

where N_0 is the number of ground state atoms per unit volume, g_k is the degeneracy of the excited state, E_k is the energy of the excited state k , k_B is the Boltzmann constant, T_e is the excited electron temperature, A_{ik} is the Einstein coefficient for the $k \rightarrow i$ transition, h is the Planck constant, and ν_{ik} is the spectral line frequency of $k \rightarrow i$ transition.

For two lines with wavelengths λ_1 and λ_2 from the same atom, the ratio of their intensities should satisfy:

$$\frac{I_1}{I_2} = \frac{A_1}{A_2} \frac{g_1}{g_2} \frac{\lambda_2}{\lambda_1} e^{-(E_1 - E_2)/k_B T_e} \quad (6)$$

where, A_1 and A_2 are the Einstein coefficients for corresponding transitions, g_1 and g_2 are the degeneracies of two excited states, and E_1 and E_2 are the energy gaps for two transitions. The double spectral line method expressed as Eq. (6) can usually be used to calculate electron temperature T_e ¹².

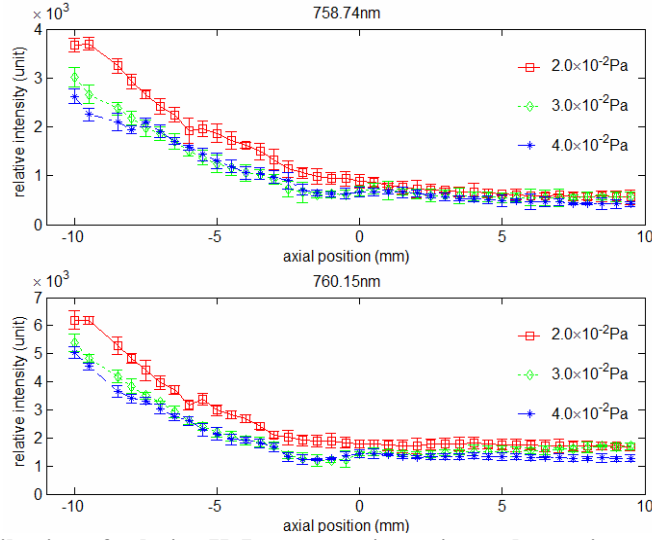


Figure 9. Axial distribution of relative KrI spectrum intensity under various vacuum backpressures

To reduce the effect of spectral transmittance and radiance on the measurements, two lines with a relatively small difference in wavelength have been chosen to calculate the electron temperature. The two spectral lines appearing at wavelengths of 758.74 nm and 760.15 nm, corresponding to

$4p^5(2P_{3/2}^o)5p^2[1/2]_0 \rightarrow 4p^5(2P_{3/2}^o)5s^2[3/2]_1^o$ and $4p^5(2P_{3/2}^o)5p^2[3/2]_2 \rightarrow 4p^5(2P_{3/2}^o)5s^2[3/2]_2^o$, respectively¹³, can be measured along the channel axis, as shown in FIG. 9.

According to Eq. (6), the axial distribution of electron temperature under various backpressures can be calculated as shown in FIG. 10, using the data of relative KrI spectrum intensity presented in FIG. 9, and the Einstein coefficients, the degeneracy of excited state, the energy gaps between considered levels provided by NIST database¹⁴.

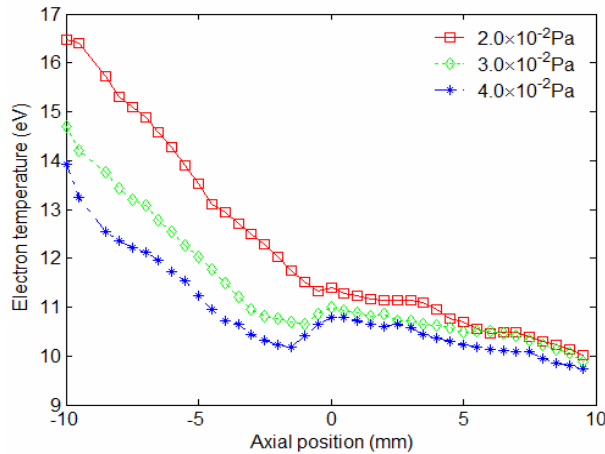


Figure 10. Axial distribution of electron temperature under various vacuum backpressures

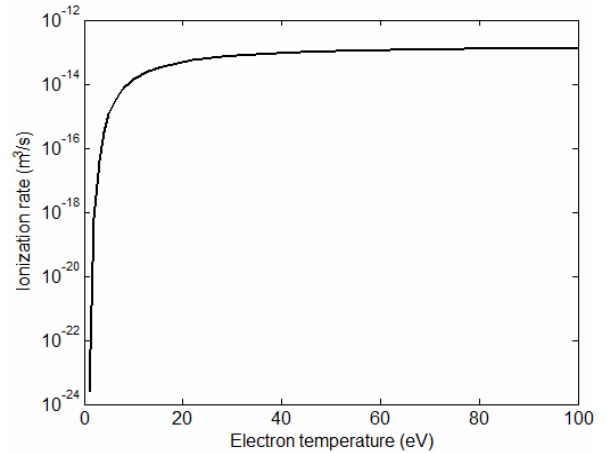


Figure 11. Ionization rate calculated with a Maxwellian electron distribution function¹⁵

It can be seen from FIG. 10 that:

1) The electron temperature decreases in the channel as the vacuum chamber backpressure increases. This result suggests that the ionization energy loss has increased with the backpressure, so the electrons can be cooled when the background gas atoms become ionized in the channel, thereby lowering the electron temperature.

2) There is a relatively low electron temperature zone near the exit, especially for the backpressures of 3.0×10^{-2} Pa and 4.0×10^{-2} Pa, and the penetration of this zone into the channel increases with the backpressure. This result is likely due to the fact that the presence of reflux gas significantly lowers the electron temperature around the exit, and the position of the valley can be regarded as the center of the reflux ionization zone. The reflux

flow rate increases with the backpressure, so the resulting electron density enhances the ionization efficiency of the reflux. The decreased electron temperature will have a greater impact on the ionization of propellants since the ionization efficiency exhibits an exponential growth with the electron temperature in the low- temperature range (FIG. 11), but only a linear growth with the electron density. Thus, the mean free path of the reflux gas atoms becomes longer, and causes the deeper ionization of reflux atoms in the channel, as shown in FIG. 8.

3) The reflux flow can have such a global effect on the electron temperature in the channel that not only the electron temperature in the vicinity of reflux ionization region, but also the mainstream ionization region deep inside the channel are affected. Since the monovalent ionization energy of Kr is 14.02 eV, it can be seen from FIG. 11 that if the electron temperature in the mainstream ionization zone is lower than this energy threshold, the ionization efficiency of Kr gas will drop dramatically.

IV. Conclusions

It can be concluded from the results and discussions above that the backpressure has a decisive influence on the discharge characteristics of Hall thrusters. Backpressure influences the mass flow rate of the background gas in the discharge channel, thereby affecting the ionization, acceleration and other physical processes of the working gas. The relative intensities of Kr, Kr⁺ emission spectrum line along the channel and the energy distribution of exhausted ions are measured in accordance with the emission characteristics of Kr, Kr⁺ and the energy distribution of the ion flow, which denotes the processes of Kr gas ionization and acceleration, respectively. The experimental results indicate that the reflux of background gas has a global effect on the discharge characteristics of the working gas. Electron temperature and working gas ionization efficiency in the channel decrease as the backpressure increases. A new ionization zone can be formed near the exit, and the penetration of the new ionization region into the channel is deeper when the vacuum backpressure is higher.

Acknowledgements

This research was funded by the Project of NSFC (Grant No. 50877018) and the Program for National Fundamental Research (No. EDAQ27206001). We would like to thank Prof. Yajun Zhou for her fruitful advices, and Ting Li, Liguang Jiao, Jingjing Yang, Ke Han and Hong Li for their technical support. The authors are most grateful to Prof. Xiaogang Wang from Peking University for providing valuable guidance and assistance during the writing of the paper.

References

- ¹ F. Hegeler, G. Masten, G. Leiker, H. Krompholz, M. Kristiansen, Proceedings of the 9th IEEE Pulsed Power Conference, Albuquerque, NM, edited by R. White and K. Prestwich (Institute of Electrical and Electronics Engineers, New York, 1995), Vol. 1, p. 237.
- ² T. Randolph, V. Kim, H. Kaufman, K. Kozubsky, V. V. Zhurin, and M. Day, Proceedings of the 23rd International Electric Propulsion Conference, Seattle, WA, edited by J. Brophy (Electric Rocket Propulsion Society, Worthington, Ohio, 1993), Vol. 01, p. 95.
- ³ R. R. Hofer, P. Y. Peterson, and A. D. Gallimore, Proceedings of the 27th International Electric Propulsion Conference, Pasadena, CA, edited by Electric Rocket Propulsion Society (Cleveland, OH, 2001), Vol.01, p. 45.
- ⁴ M. L. R. Walker, University of Michigan, 2005.
- ⁵ M. L. R. Walker, A. L. Victor, R. R. Hofer, and A. D. Gallimore, Journal of Propulsion and Power 21, 408 (2005).
- ⁶ A. D. Gallimore, M. M. L. Walker, B. E. Beal, and T. B. Smith, (University of Michigan, 1996).
- ⁷ A. I. Morozov and V. V. Savelyev, Reviews of Plasma Physics (Consultants Bureau, New York, 2000).
- ⁸ A. I. Bugrova, A. V. Desyatskov, A. I. Morozov, and V. K. Kharchevnikov, Plasma Physics Reports 26, 715 (2000).
- ⁹ L. Yuquan and Y. Daren, Plasma Science and Technology 8, 666 (2006).
- ¹⁰ K. Dzierzega, U. Griesmann, and G. Nave, Physica Scripta 63, 209 (2001).
- ¹¹ A. P. Thorne, Spectrophysics (Chapman and Hall, London, 1974).
- ¹² R. L. Mills, P. C Ray, M. Nansteel, C. Xuemin, R. M. Mayo, H. Jiliang, and B. Dhandapani, IEEE Transactions on Plasma Science 31, 338 (2003).
- ¹³ S. Tsurubuchi, H. Kobayashi, and M. Hyodo, Journal of Physics-London-B Atomic Molecular and Optical Physics 36, 2629 (2003).
- ¹⁴ E. B. Saloman, and NIST ASD Team, NIST Atomic Spectra Database (version 3.1.4), NIST, Gaithersburg, MD, 2008.
- ¹⁵ L. Garrigues, I. D. Boyd, and J. P. Boeuf, Journal of Propulsion and Power 17, 772 (2001).